

Design Optimization of Conformal Antennas by Integrating Stochastic Algorithms With the Hybrid Finite-Element Method

Zhifang Li, *Member, IEEE*, Yunus E. Erdemli, *Member, IEEE*, John L. Volakis, *Fellow, IEEE*, and Panos Y. Papalambros

Abstract—Previous work in antenna optimization has primarily focused on applications of optimization algorithms in conjunction with problem-specific or semi-analytic tools. However, recent developments in fast algorithms now offer the possibility of designs and moreover allow for full flexibility in material specification across three dimensions. As an example, this paper combines genetic algorithms (GA) and simulated annealing (SA) with fast hybrid finite-element boundary integral simulations to develop full three-dimensional (3-D) antenna designs using shape, topology, as well as material optimization. To illustrate these optimization methods as well as compare between GA and SA, three different antenna designs are considered. First, a folded-slot antenna is optimized for broad-band performance, followed by an irregular-shaped dual-band antenna design. As a third design, which combines shape and material optimization, a bandgap substrate is designed to substantially increase the bandwidth of a patch residing on the optimized substrate.

Index Terms—Antennas, electromagnetic bandgap structures, design optimization, periodic substrates.

I. INTRODUCTION

FREQUENCY-selective volumes (FSVs) and electromagnetic bandgap (EBG) structures have emerged as a new multidisciplinary field of study [1], [2]. A bandgap structure consists of composite materials where certain dielectric or metal sections are implanted (possibly periodically) within a background medium. In analogy to semiconductor crystals which may exhibit an electronic bandgap, in electromagnetics such bandgap structures are associated with a frequency band where propagation of electromagnetic (EM) waves is forbidden and may also be used to modify the reflective properties of multilayered structures. These features may be exploited in the design of EM devices. In the case of antennas, bandgap substrate consists of printed elements on periodic, or more generally, on some perforated substrates which can be designed to enhance antenna properties such as bandwidth and pattern. Parameters which affect the behavior of EBGs include their periodicity, shape and

spacing of the implants, and the dielectric contrast between the composite materials.

Growing applications in wireless communications present us with continuing demands for new antenna designs. Various antenna features and performance metrics are desired, including miniaturization, pattern control, new composites and artificial dielectrics, and multifunction capabilities. Antenna design is therefore a topic of great importance to electromagnetics. It involves the selection of antenna physical parameters to achieve optimal gain, pattern performance, voltage standing-wave ratio (VSWR), bandwidth, and so on, subject to some specified constraints. Trial and error process is typically used for antenna design and consequently the designer is required to have great experience and intuition.

Recently, optimization methods have been introduced for antennas aimed at either improving the current design or at speeding up the design process [3]–[5]. The combination of various optimization methods and numerical techniques such as the method of moments (MoM) further enables the optimization of complicated patch antennas and layered EM devices [6]–[8]. Creation of irregular patch and frequency-selective surface (FSS) shapes have also been investigated for various purposes. Previous work includes Q -factor improvements using a combination of finite-difference time-domain (FDTD) and genetic algorithms (GA) [5], and bandwidth improvement for patch antennas [3] and FSS shape design for microwave absorbers [9] with MoM and GA.

In this paper, we integrate design optimization methods with robust finite-element boundary-integral (FE-BI) methods for printed antenna design without limitations on antenna shape and topology, or substrate material distribution. To our knowledge, this is the first ever integration of optimization and rigorous FE-BI analysis tools, and the first paper to optimize three-dimensional (3-D) material distribution of a bandgap substrate for enhancing antenna bandwidth. A key element of this integration is the use of new fast algorithms recently introduced in the FE-BI formulation [10], [11]. For design optimization we use the standard GAs, but we also considered other stochastic design approaches such as the simulated annealing (SA). A comparison of the two techniques is also given.

This paper is organized as follows. Section II outlines GA and SA and how these methods work with the FE-BI solver. In Section III, we propose two design examples based on shape/topology optimization to serve as design practice and verification of the optimization process and integration with

Manuscript received August 17, 2001; revised February 28, 2002.

Z. Li is with Guidant Corporation, St. Paul, MN 55112 USA (e-mail: zhi-fang@umich.edu).

Y. E. Erdemli and J. L. Volakis are with the Department of Electrical Engineering and Computer Science, University of Michigan, Ann Arbor, MI 48109-2122 USA (e-mail: yunusee@umich.edu; volakis@umich.edu).

P. Y. Papalambros is with the Department of Mechanical Engineering, The University of Michigan, Ann Arbor, MI 48109-2125 USA (e-mail: pyp@umich.edu).

Publisher Item Identifier S 0018-926X(02)05461-3.

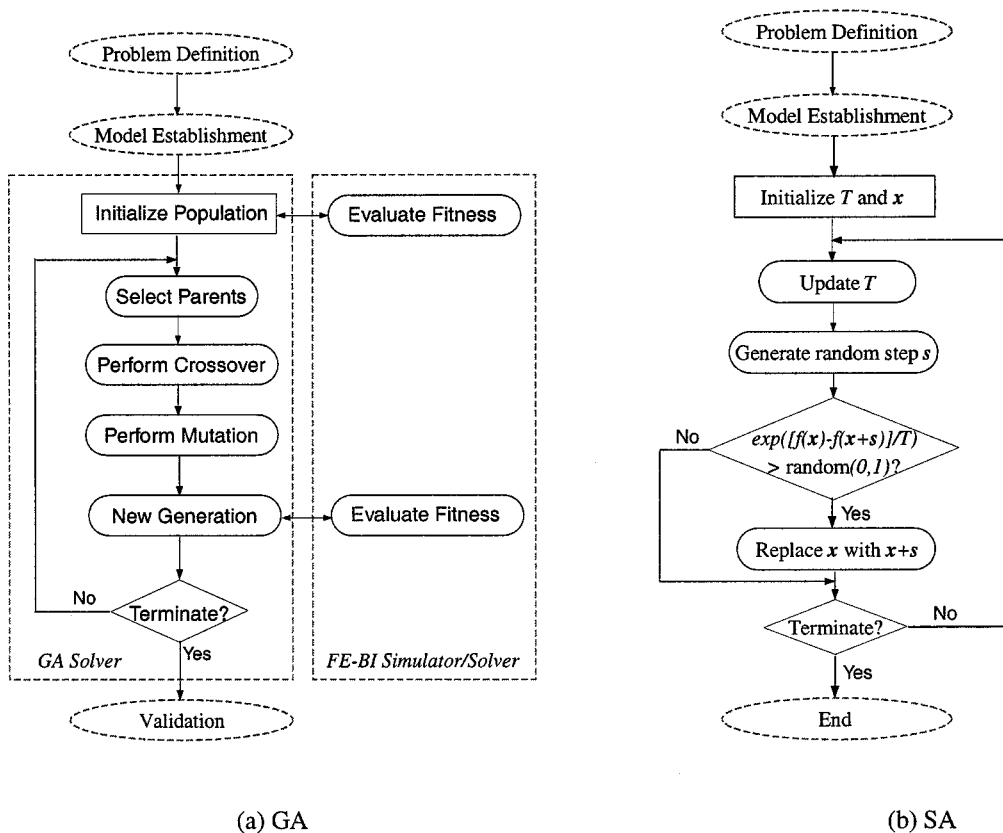


Fig. 1. General optimization process using GA or SA and an FEM solver.

exact computational tools. The examples include 1) a patch design with a folded-slot feed for increased bandwidth and 2) a dual band patch where we also take the opportunity to compare GA and SA performance. In Section IV, we consider a full 3-D design where the emphasis is on material design. In this case, a bandgap structure is designed to serve as the substrate for the patch subject to prespecified bandwidth requirements.

II. OPTIMIZATION METHODS AND EM ANALYSIS TOOLS

For the past several decades, gradient-free methods (a class of optimization methods which do not use derivative information but instead rely only on function values) have been introduced to search for global optima. Gradient-free methods [12], or direct-search methods, are generally robust and particularly effective for problems with a large number of design variables, but typically require fast objective function evaluations for their practical implementation. They are largely independent of the initial design and solution domain. Therefore, global optima are more likely to be found. As can be understood, gradient-free methods work very well when many local optima exist, whereas gradient-based methods [13], [14] break down in these cases. On the other hand, gradient-free methods are generally slow and require a large number of objective function evaluations to achieve convergence. Hence, they have limited use in problems involving complicated electromagnetic structures where traditional numerical simulations must be used for the objective function computation. Recent fast integral algorithms and their integration with finite-element methods make the use of

such gradient-free optimizations more practical. This paper focuses on the integration of GA and SA with exact FE-BI analysis tools, and demonstrates design possibilities using full 3-D antenna models comprised of composite materials.

In what follows, we begin by briefly discussing the GA and SA algorithms and their integration with the FE-BI solver. We then proceed to use GA and SA with exact FE-BI tools for printed antenna design.

A. GAs

As discussed above, GA are robust, stochastic-based search methods modeled on the concepts of natural selection and evolution, and their underlying process has already been discussed [15], [16]. There are two basic types of operators for GA. The *crossover* operator swaps parts of two solutions to generate two new solutions and the *mutation* operator randomly changes a small percentage of bits in chromosomes, from 1 to 0 or *vice versa*. The flowchart for a GA process is shown in Fig. 1(a). In the beginning, a desired performance is described and formulated as a fitness function $f(x)$ to be minimized by the GA optimizer, where x is a vector of design variables (e.g., yes or no metallization of each pixel in the design domain, yes or no on the use of dielectric at certain locations, etc.). If the optimization model contains constraints, they can be included as penalties in the fitness function or encoded directly into the solution strings. Several initial designs coded into binary strings are produced for the first generation either by the user or randomly. For each design, the fitness values are computed using the FE-BI solver and rated. Good solutions survive and have offsprings, while bad

solutions are discontinued. Pairs of good solutions are selected using certain strategies to perform crossover. Mutation is usually allowed with a very small probability to flip some bits from 0 to 1 in the binary string and *vice versa*, thus providing a way to introduce new designs. This process is repeated until the termination criteria are met. Then the optimal binary string is decoded back into the corresponding design. In GA, local optima are avoided by hyperplane sampling in the Hamming space (i.e., crossovers) plus random perturbations (i.e., mutations) [17].

Both the FE-BI and GA codes were written in Fortran. For each specific problem, an interface code is also written to communicate between these two parts. The interface code reads in the initial population, translates them into the values of design variables, and inputs these variables to the FE-BI code for meshing and solving. The fitness function (i.e., objective function) is computed and sent to the GA code, which performs crossover and mutation accordingly. New generation is then formed and design variables are updated for the fitness evaluation again. For all the three optimization problems in this paper, a micro-GA is used with a tournament selection strategy (a widely used class of selection mechanisms that pick k members of the population at random and then select from them in a manner that depends on a fitness criterion), with a shuffling technique for choosing random pairs for crossover. Uniform crossover with a crossover probability of 0.5 was used in conjunction with a mutation probability of 0.02. A population of five is formed in each of the GA generation. Convergence are typically achieved within 150 generations.

B. Simulated Annealing

Simulated annealing [18], [19] was proposed by Kirkpatrick *et al.* in 1983 [20]. SA is a stochastic hill-climbing algorithm based on an analogy with the physical process of annealing. In physics of condensed matter, annealing is known as “a thermal process for obtaining low-energy states of a solid in a heat bath” [18]. The process contains two steps.

- Increase the temperature to a value at which the solid starts to melt. In this liquid state, all particles arrange themselves randomly.
- Decrease the temperature slowly until the particles arrange themselves in the ground state of the solid. In this ground state, the particles are arranged in a highly structured lattice and the system energy is minimal.

To achieve the ground state, the melting temperature must be sufficiently high and the cooling is done sufficiently slow. One must use an annealing process, where the temperature of the system is elevated, and then gradually lowered, spending enough time at each temperature to reach thermal equilibrium. If insufficient time is spent at any temperature, especially near the freezing point, the solid will be frozen into a meta-stable state called *quenching*.

To apply SA to optimization problems, proper analogues must be identified between the SA and physical annealing: the energy equation becomes the objective function, the current state of the thermodynamic system becomes the iterate solution, ground state becomes the global minimum, and temperature becomes the control parameter for the process.

Briefly, SA works in the following manner to minimize an objective function $f(\mathbf{x})$ [see Fig. 1(b) for the flowchart].

- 1) Start with a feasible initial point \mathbf{x}_0 and temperature $T = T_0$.
- 2) Generate a new point $\mathbf{x}_{k+1} = \mathbf{x}_k + \mathbf{s}_k$, where \mathbf{s}_k is the step size (e.g., $\mathbf{s}_k = 0.5\sqrt{T_k} * (\text{random}[0, 1] - 0.5)$, where $\text{random}[0,1]$ is a randomly generated number between 0 and 1).
- 3) Apply the Metropolis criterion [21] to judge $f(\mathbf{x}_{k+1})$:
if $f(\mathbf{x}_{k+1}) \leq f(\mathbf{x}_k)$, accept \mathbf{x}_{k+1} ;
otherwise, accept \mathbf{x}_{k+1} with probability

$$P = e^{(f(\mathbf{x}_k) - f(\mathbf{x}_{k+1}))/T_k}$$

or reject with probability $(1 - P)$.

- 4) Decrease temperature T according to some heuristic cooling schedule (for example, $T_{k+1} = 0.9T_k$).
- 5) Go to Step 2).

SA is similar to GA (of single-size population) when crossovers are disabled and only mutations are used. Of course, SA has its unique characteristics and cannot be seen simply as equivalent to GA. An important aspect of SA is that optimization is not always mono directional (downhill). The probabilities of accepting an uphill move and step size are determined by the value of temperature T , both of which are reduced as the temperature becomes lower. At the beginning of the SA process, T is relatively large, making the step size large and the accepting probabilities high. Thus, more designs can be explored within the domain. As SA progresses, T is lowered. Therefore, the step size is decreased and uphill moves are more likely to be rejected, constraining the search to a more “local” area. Eventually, the process settles by only accepting downhill moves. In this manner, SA prevents itself from getting stuck in inferior local optima and is more likely to settle in areas of global quality.

The disadvantage of SA is that parameter settings for the cooling schedules are very complicated and not well understood. Such parameters are the initial temperature, the relationship between step size and temperature, number of iterations at each temperature, and the temperature decrease rate at each step as cooling proceeds. Determining appropriate values for all these parameters is often accomplished through trial and error, which can become prohibitively expensive for all but the simplest problems. Similarly, although usually to a less extent, GA also bear the heuristic characteristics in choosing parameters for a specific problem, such as population size, crossover points, and mutation probability. Recently, an adaptive simulated annealing (ASA) algorithm [22] was introduced to improve the basic SA algorithm, but its study is beyond the scope of this paper.

III. DESIGN PRACTICE

In this section, two optimization design problems are investigated for the purpose of verification. First, a rectangular patch excited with a folded-slot feed is optimized for broad-band performance using GA. Later, GA and SA are compared for the design of an irregular-shaped dual-band patch antenna. We discuss the design effectiveness of both methods.

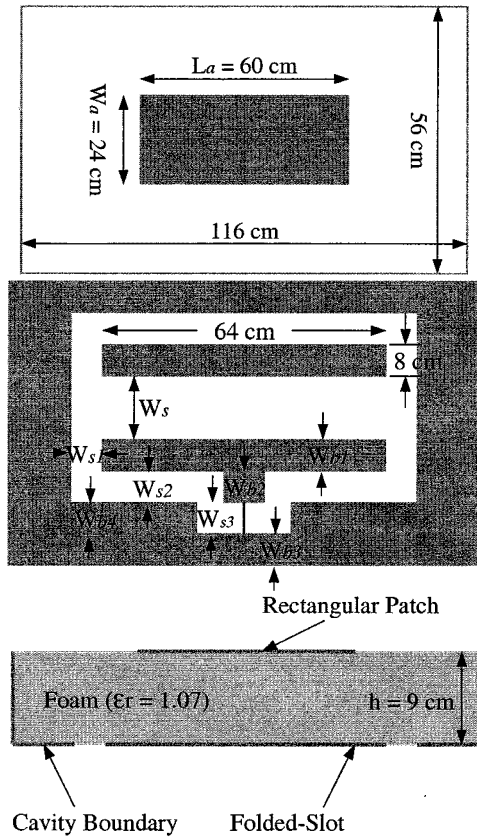


Fig. 2. Geometry of the stacked rectangular patch and folded-slot: top, bottom, and side view.

A. Patch With Folded-Slot Feed

In this section, a novel configuration of a folded-slot feed for a rectangular patch antenna is designed to achieve a 22% impedance bandwidth (as compared to the standard patch bandwidth of 2–5%). A fast hybrid FE-BI code [10] having $O(N)$ CPU requirements is used to compute the input impedance and integrate it with the GA optimizer. Finally, measured data are presented to validate the design.

One reason for considering the folded-slot feed is because it provides greater bandwidth [23] than traditional aperture-coupled slot feeds and allows for greater design flexibility. The proposed configuration is displayed in Fig. 2 and the goal is to find the optimal values for the various slot and strip widths of the folded-slot feed to achieve a 10-dB return loss over a 134–175-MHz (VHF frequencies) bandwidth with reference to a 50- Ω input impedance. Therefore, the objective function can be defined to minimize the highest return loss among several sample frequencies

$$\min \left(\max_{k=1,2,3} |S_{11}|_k \right) \quad (1)$$

where $|S_{11}|_k$ refers to the return loss at 134, 154, and 174 MHz for this problem.

The actual antenna resides in a cavity of size 116 cm \times 56 cm, and the folded slot is separated from a patch by a foam substrate with $\epsilon_r = 1.07$ and thickness $h = 9$ cm. The rectangular patch on the top is fixed at length $L_a = 60.0$ cm and width $W_a = 24.0$ cm. There is an extra metal bar of length 64 cm and width

TABLE I
VALUES OF THE FIVE DESIGN VARIABLES OF THE INITIAL AND OPTIMAL FOLDED-SLOT ANTENNAS

	W_s (cm)	W_{s2} (cm)	W_{s3} (cm)	W_{b2} (cm)	W_{b4} (cm)
Initial design	8.0	4.0	4.0	8.0	6.0
Optimal design	12.0	2.0	2.0	6.0	8.0

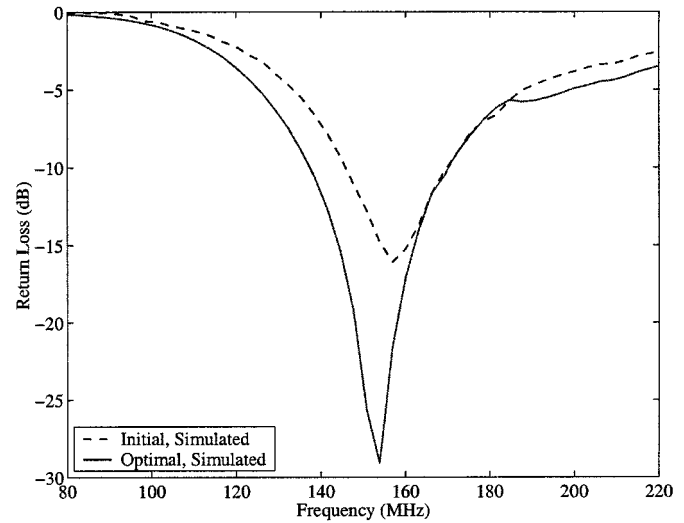


Fig. 3. Return loss of the initial and optimal folded-slot antennas.

8 cm inside the folded slot which serves to reduce the input impedance value [24].

The design variables for this optimization problem are the slot widths and positions: W_s , W_{s2} , W_{s3} , W_{b2} , and W_{b4} (see Fig. 2). For analysis, the whole antenna volume is discretized using the finite-element method (using prism elements for the volume and triangles for the surface integral) involving 44 000 edge unknowns with 7000 surface unknowns at the top boundary integral aperture. For this system size, the per-frequency CPU time is about 45–60 min on a SUN Ultra-10 workstation. Since the computation time per frequency is rather large, a continuous five-variable gradient-based optimization is not realistic. To simplify the design process, the sizes of the design variables are not allowed to change continuously, but only discretely within the fixed discretization grid of $\Delta x = 4.0$ cm and $\Delta y = 2.0$ cm. The values of the design variables for the initial and optimal designs are shown in Table I, and their performance is illustrated in Fig. 3. The optimal design has an improved 10-dB bandwidth of 22.2% (from 136 to 170 MHz), as compared to the 15.9% bandwidth of the initial design. Both the initial and optimal designs were fabricated and measured. Fig. 4 shows the measured data of the optimal design. As seen, they are in excellent agreement with our simulations, thus verifying the analysis and design methods.

B. Irregular-Shaped Dual-Band Patch

For personal communications, multiband antennas are of particular interest. Here we consider a dual-band antenna design using a single patch. As above, the design will be carried out

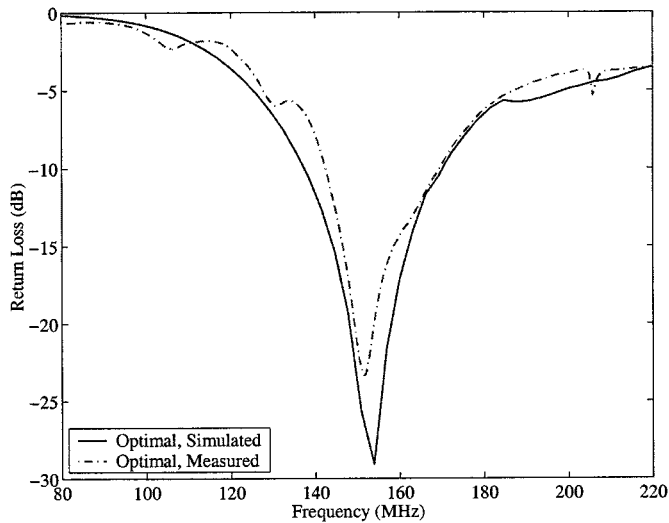


Fig. 4. Measured and simulated return loss of the optimal folded-slot antenna.

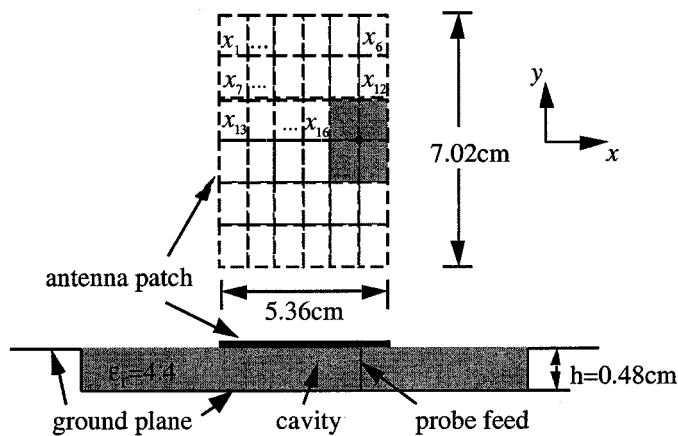


Fig. 5. Top and side view of the dual frequency design domain.

by combining an optimizer with an FE-BI solver. A relevant application is to design a patch that operates at the two GPS frequencies: 1227 and 1572 MHz, and it is appropriate to adapt a symmetric patch configuration. As shown in Fig. 5, the design domain has a size of 5.36 cm \times 7.02 cm, residing on top of a cavity 10.72 cm (along x -axis) \times 14.04 cm (along y -axis) above a substrate of thickness 0.48 cm and a dielectric constant $\epsilon_r = 4.4$. This region is discretized using 6 \times 6 rectangular grids, which are treated as design variables. Each variable is allowed to be either filled ($x_i = 1$) or empty ($x_i = 0$), although the four elements in the middle-right part of the domain are always filled with metal in order to fix the feed point. Also, due to the symmetry requirement, only the upper half of the domain needs to be considered. Therefore, we have 16 design variables x_1, x_2, \dots, x_{16} . The objective function of this problem is chosen to be

$$\min_x (|S_{11}|_1 + 0.1 * |S_{11}|_2 + |S_{11}|_3) \quad (2)$$

where $|S_{11}|_k$, for $k = 1, 2, 3$, refers to the return loss at three sample frequency points (1227, 1400, and 1573 MHz in this case). With such an objective function, more weight is placed on $|S_{11}|_1$ and $|S_{11}|_3$, and less weight is placed on $|S_{11}|_2$, therefore pushing the design to be dual-resonance rather than broad-band. We remark that this objective function can be combined with

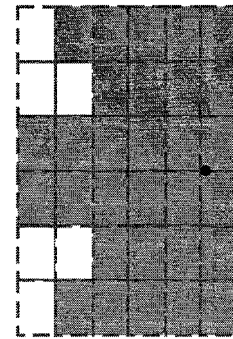


Fig. 6. Optimal design of the patch for dual-frequency operation.

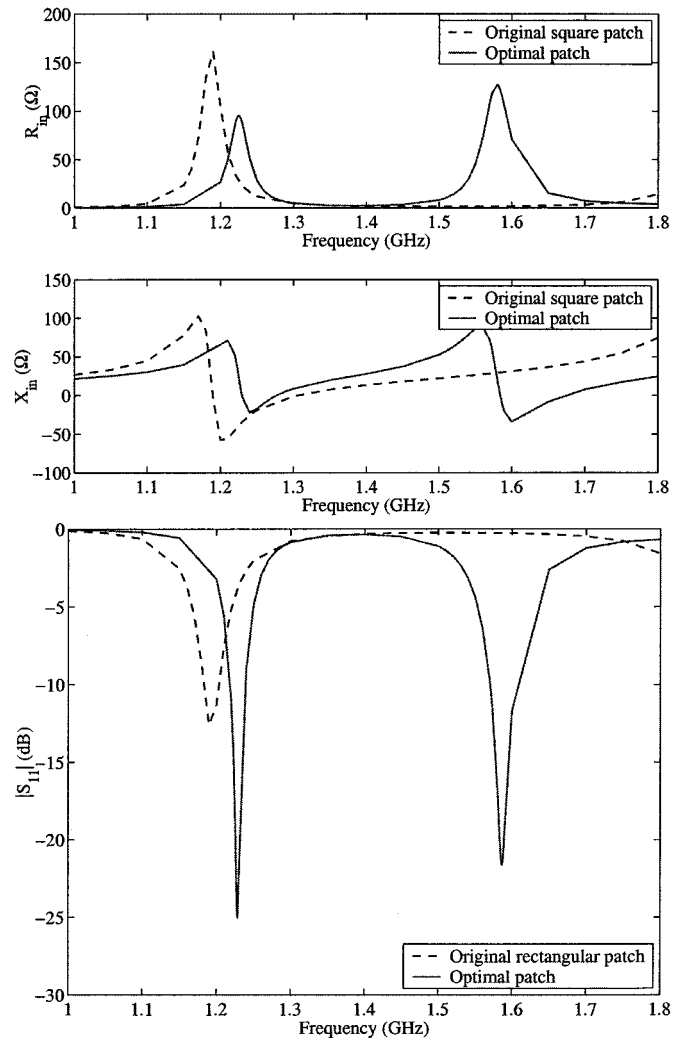


Fig. 7. Input impedance and impedance bandwidth of the original and optimal dual-frequency patches.

other criteria based on polarization and pattern requirements. However, at this point our focus will be only on the optimization of the return loss.

For comparison purposes, both GA and SA optimizers are separately applied to this design problem. Both methods generate the same optimal configuration shown in Fig. 6, whereas the corresponding impedance and return loss are shown in Fig. 7. As per design, the resonant frequencies of the optimized patch occur at both 1225 and 1571 MHz. However, the iteration

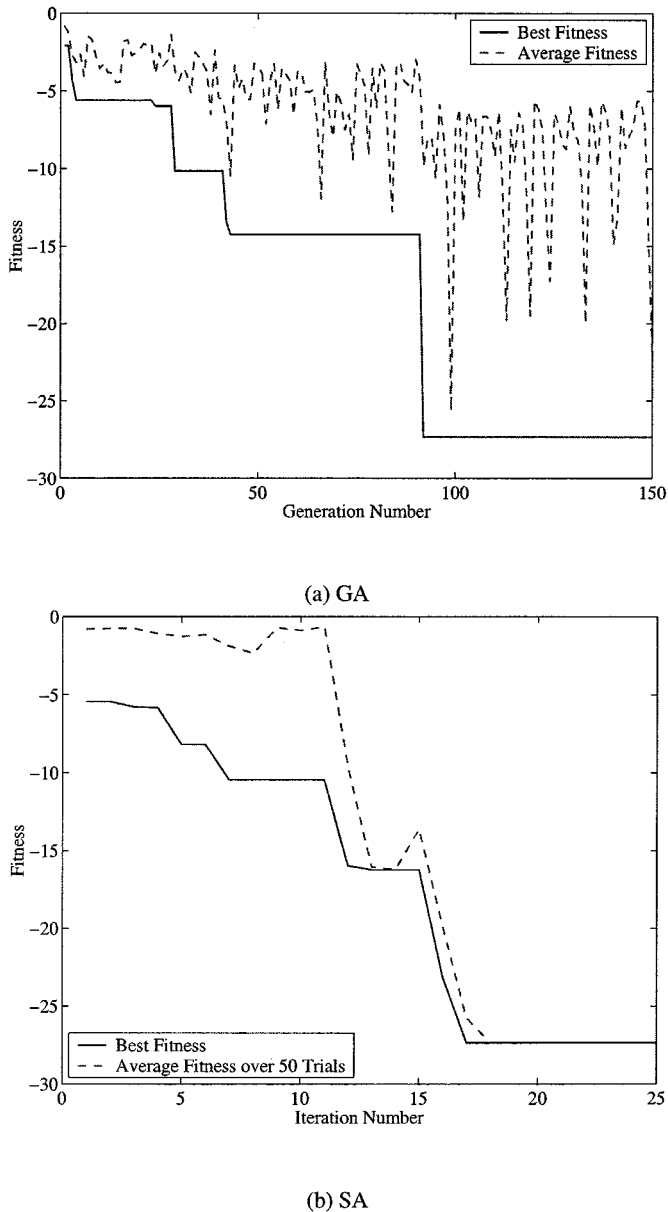


Fig. 8. Iteration history of GA and SA for the dual-frequency patch design.

histories for the GA and SA runs are quite different. Although GA and SA obtained the same optimal design, Fig. 8 shows that the GA algorithm finished at the 460th simulation (i.e., at the 92nd generation with a population size of five for each generation), whereas the SA took 850 simulations (50 trials over each of the 17 temperatures before convergence) to reach the same design. That is, the GA algorithm converged in nearly half the number of iterations (and CPU time) as compared to the SA algorithm. This might be caused by the selection of SA parameters such as step size, temperature decreasing rate, and the number of iterations at each temperature. If a different set of SA parameters are chosen to run this problem, the convergence speed might change. This is the disadvantage of SA, i.e., heavy reliance on parameters for the cooling schedule.

We close this section by noting that the proposed design was based on an objective function which only dealt with frequency tuning, but for this application a feed must also be designed

for CP radiation. The latter was not discussed since it not was included as part of the design objective, but can be included either as a concurrent or a second step optimization.

IV. MATERIALS DESIGN

It is fair to state that shape (and even some topology) optimization has been extensively exploited for printed antenna design. However, designs utilizing full 3-D topology and material optimization have yet to be considered. It represents the only remaining parameter for developing novel electromagnetic devices and recent experience with bandgap substrates indicates that materials offer much potential for design. In this section, we show for the first time how designs based on periodic material substrates can lead to significant increases in patch antenna bandwidth.

Previous works have shown that bandgap substrates surrounding a patch antenna can be used to suppress surface waves [25]. However, considerable area is required around the patch antenna (on the order of at least three wavelengths [26]) to accomplish this. Here we will consider a periodic substrate design which lies under the patch for bandwidth enhancement. Since it is reasonable to assume that bandwidth enhancement will occur near the resonance of the bandgap structure, we will first consider a bandgap layer such as that shown in Fig. 9 and work around the bandgap frequency. This slab has a background $\epsilon_r = 4$ and a unit cell size of $2 \text{ cm} \times 2 \text{ cm}$. The embedded periodic material blocks have $\epsilon_r = 10$ and a size of $1 \text{ cm} \times 1 \text{ cm}$. For this structure, the size of the periodic implants is a significant fraction of a wavelength. Therefore, a homogeneous ϵ_r cannot be used for modeling purposes. Instead, the substrate must be modeled exactly with different ϵ_r s at each substrate location, necessitating use of the finite-element method for material modeling. For our purposes, we used a special periodic FE-BI solver [10] for the analysis of 3-D doubly periodic structures having arbitrary material composition. Fig. 10 shows the reflection coefficient curve at normal incidence and as seen, the effective medium theory (with a homogenized $\epsilon_r = 5.5$) fails to predict the resonance at the bandgap frequency around 10–11 GHz [27]. This curve also shows that operation should be around 10 GHz to exploit the bandgap property of this periodic substrate.

Given the above discussion, we proceed to set the following optimization goals after placing a patch on top of the bandgap substrate (see Fig. 11):

- optimize patch height (air layer) Δ ,
- optimize the bandgap block shape,

to achieve an impedance bandwidth of 15% with center frequency around 10.5 GHz.

For our design using GA, we choose a design domain comprised of 3×3 unit cell block configuration with the patch located at the center of the domain as shown in Fig. 11. In actuality, the design domain is only $1/9$ of the substrate by exploiting symmetry and periodicity, but the simulation is carried out on the whole domain since the substrate is now finite. The objective function of this optimization problem is

$$\min_{\mathbf{x}} \left(\max_{k=1, 2, \dots, 5} |S_{11}|_k \right) \quad (3)$$

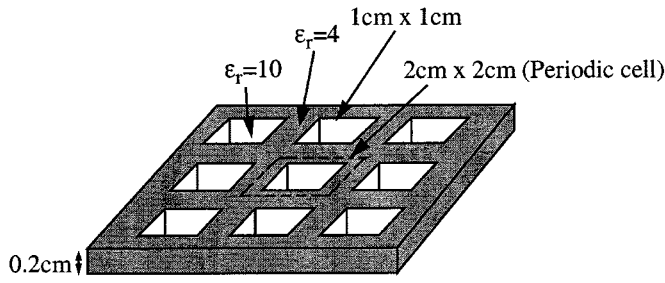


Fig. 9. Geometry of the infinite bandgap structure.

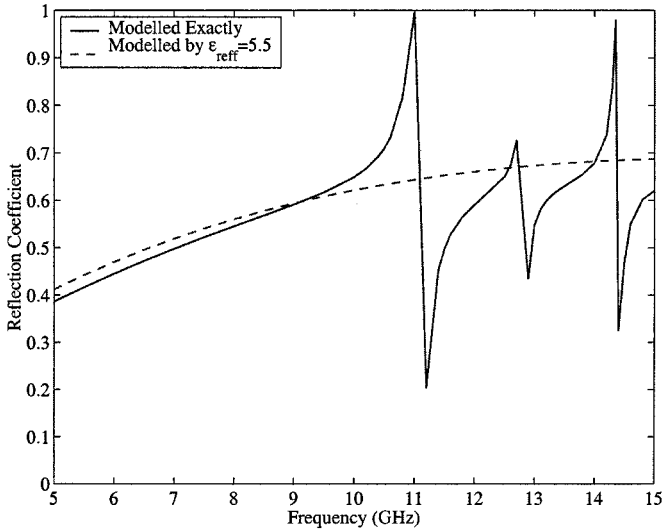


Fig. 10. Plane-wave reflection from the bandgap structure shown in Fig. 9, using exact modeling and effective constant modeling.

where $|S_{11}|_k$ refers to the return loss at five sample frequency points (10.2, 10.4, 10.6, 10.8, and 11.0 GHz in this case) defined as

$$|S_{11}| = \frac{|Z_{in} - Z_0|}{|Z_{in} + Z_0|} \quad (\text{dB}) \quad (4)$$

where Z_{in} is the input impedance at the feed and $Z_0 = 50 \Omega$. By minimizing the highest $|S_{11}|$ among the five, we could reduce the difference between the highest and lowest $|S_{11}|$'s, therefore achieving a larger bandwidth [3].

The original bandgap substrate (i.e., 3×3 square-shaped dielectric blocks with $\epsilon_r = 10$ implanted in an $\epsilon_r = 4$ medium, whose discretization is shown in Fig. 12) gave the $2 \text{ cm} \times 2 \text{ cm}$ patch a typical 10-dB bandwidth of 3%. This original design is used by the GA optimizer as one of the five initial designs. Each GA generation consists of five designs, with five frequencies computed for each design. On an HP 900-785 workstation, each generation takes about 30 min to finish. The optimal block configuration for the bandgap substrate is shown in Fig. 13, separated by an air layer $\Delta = 0.1 \text{ cm}$ from the patch. The achieved impedance and return loss of the optimal design show a 10-dB bandwidth of 17.7% (see Fig. 14). From this, it is clear that the various material combinations such as frequency selective volumes (FSVs) and frequency selective surfaces (FSSs) when used as substrates may have a significant effect on antenna bandwidth performance.

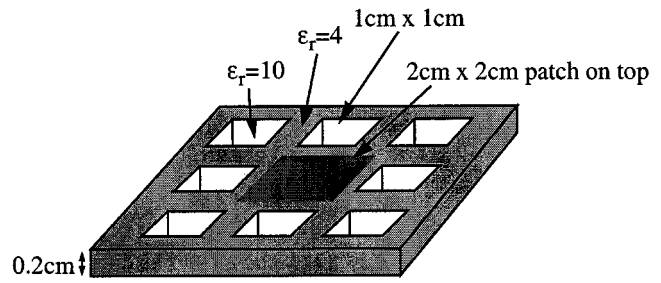


Fig. 11. Geometry of the cavity-backed patch over finite bandgap structure.

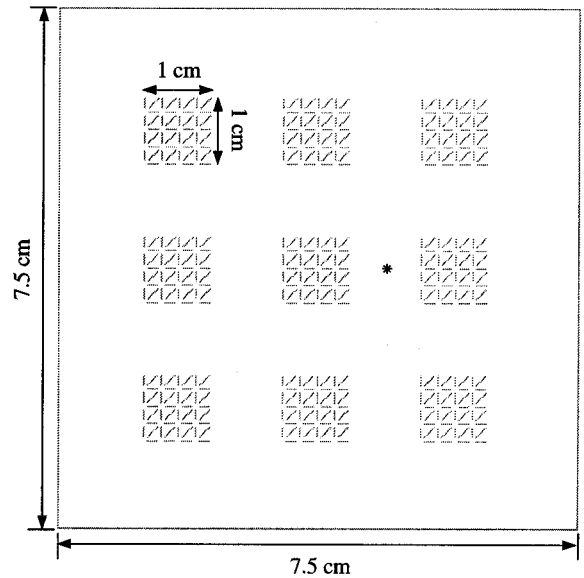
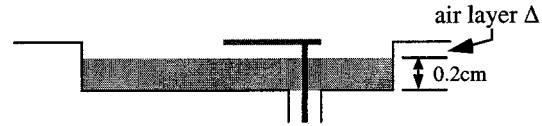


Fig. 12. Initial 3-D block configuration for the bandgap substrate: top view. "*" marks the location of feed point.

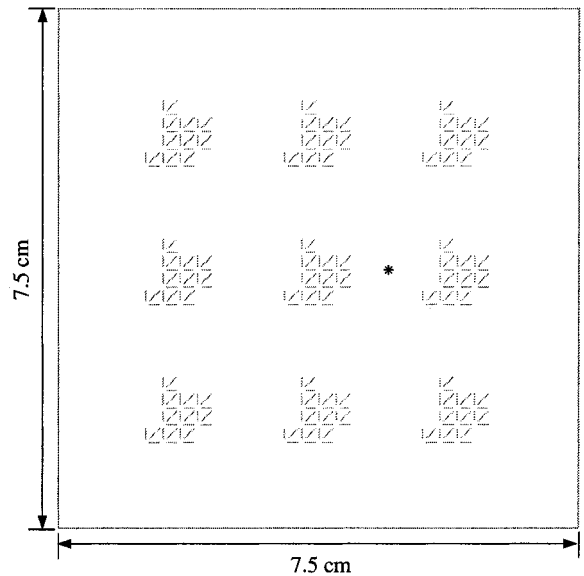


Fig. 13. Optimal 3-D block configuration for the bandgap substrate: top view. "*" marks the location of feed point.

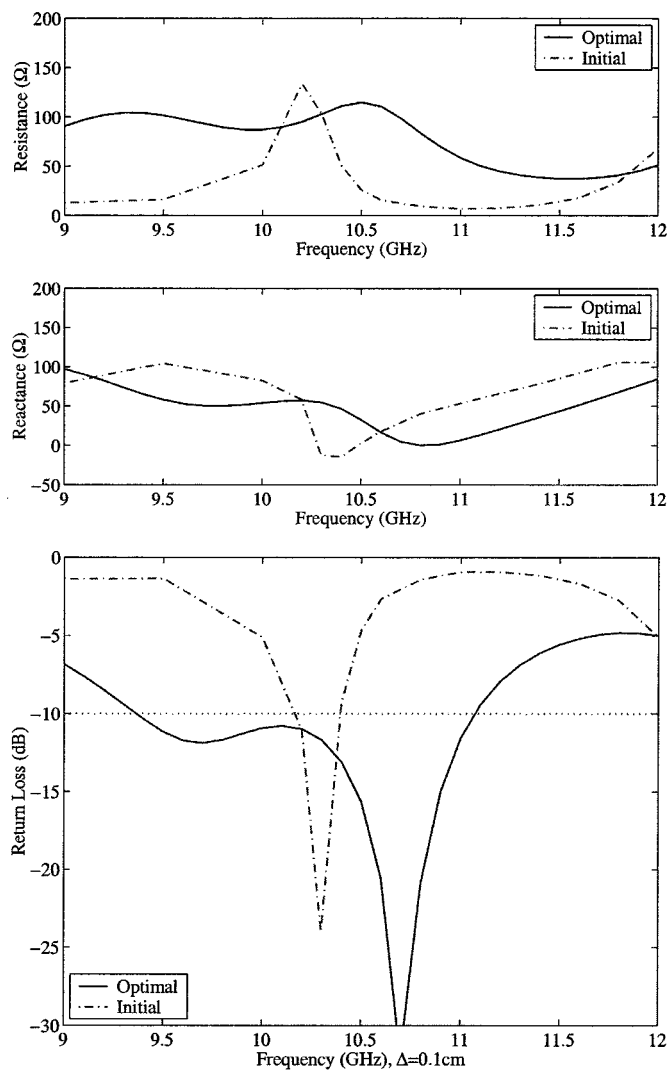


Fig. 14. Input impedance and return loss of the cavity-backed patch over bandgap structure with and without air layer.

V. CONCLUSION

Two stochastic design algorithms, one based on a genetic algorithm and the other on simulated annealing were integrated with a FE–BI solver to demonstrate full flexibility in designing antennas by combining shape, topology and material optimization. Of importance in generating such designs is the use of fast $O(N)$ or $O(N \log N)$ algorithms in carrying out the hundreds and possibly thousands of solver calls within the design loop. In this paper, we demonstrated the integration of robust design and solver algorithms for three antenna applications having bandwidth and multiband operational objectives. The first two applications concentrated on size and shape optimization, and served as verifications of the integration process and design practice. They included: 1) a rectangular patch fed by a folded slot which was optimized to achieve a 22% bandwidth; and 2) a dual-frequency patch, designed using both GA and SA algorithms. The latter design was used for comparing the effectiveness and efficiency of GA and SA, with the conclusions that although both generated the same antenna shape, GA was found to be faster than SA.

The third optimization example, demonstrated the full 3-D capability of the design approach by concurrently exploiting both shape and material optimization to enhance the bandwidth of a simple rectangular patch on a bandgap substrate. For this case, the design algorithm generated a substrate which combined two layers, one of which was occupied by the bandgap structure whose material implants were nonrectangular and irregularly shaped. The delivered bandwidth using this substrate is a remarkable 17%. This would indicate that the designed substrate is likely to behave similar to a magnetic ground plane near the operational frequencies where the antenna shows its best bandwidth performance.

REFERENCES

- [1] J. D. Joannopoulos, R. D. Meade, and J. N. Winn, *Photonic Crystals: Molding the Flow of Light*. Princeton, NJ: Princeton Univ. Press, 1995.
- [2] A. S. Barlevy and Y. Rahmat-Samii, "Characterization of EM band-gaps composed of multiple periodic tripods with interconnecting vias: concept, analysis and design," *IEEE Trans. Antennas Propagat.*, vol. 49, pp. 343–353, Mar. 2001.
- [3] J. M. Johnson and Y. Rahmat-Samii, "Genetic algorithms and method of moments (GA/MoM) for the design of integrated antennas," *IEEE Trans. Antennas Propagat.*, vol. 47, pp. 1606–1614, Oct. 1999.
- [4] F. Ares, S. R. Rengarajan, E. Villanueva, E. Skochinski, and E. Moreno, "Application of genetic algorithms and simulated annealing technique in optimising the aperture distributions of antenna array patterns," *Electron. Lett.*, vol. 32, pp. 148–149, Feb. 1996.
- [5] C. Delabie, M. Villegas, and O. Picon, "Creation of new shapes for resonant microstrip structures by means of genetic algorithms," *Electron. Lett.*, vol. 33, pp. 1509–1510, Aug. 1997.
- [6] L. Alatan, M. I. Aksun, K. Leblebicioglu, and M. T. Birand, "Use of computationally efficient method of moments in the optimization of printed antennas," *IEEE Trans. Antennas Propagat.*, vol. 47, pp. 725–732, Apr. 1999.
- [7] Z. Li, P. Y. Papalambros, and J. L. Volakis, "Designing broad-band patch antennas using the sequential quadratic programming method," *IEEE Trans. Antennas Propagat.*, vol. 45, pp. 1689–1692, Nov. 1997.
- [8] C. Zuffada, T. Cwik, and C. Ditchman, "Synthesis of novel all-dielectric grating filters using genetic algorithms," *IEEE Trans. Antennas Propagat.*, vol. 46, pp. 657–663, May 1998.
- [9] S. Chakravarty, R. Mittra, and N. R. Williams, "On the application of the microgenetic algorithm to the design of broad-band microwave absorbers comprising frequency-selective surfaces embedded in multilayered dielectric media," *IEEE Trans. Microwave Theory Tech.*, vol. 49, pp. 1050–1059, June 2001.
- [10] T. F. Eibert and J. L. Volakis, "Fast spectral domain algorithm for hybrid finite element/boundary integral modeling of doubly periodic structures," *Inst. Elect. Eng. Proc.: Microwaves, Antennas Propagat.*, vol. 147, pp. 329–334, Oct. 2000.
- [11] S. S. Bindiganavale, J. L. Volakis, and H. Anastassiou, "Scattering from planar structures containing small features using the adaptive integral method (AIM)," *IEEE Trans. Antennas Propagat.*, vol. 46, pp. 1867–1878, Dec. 1998.
- [12] R. Horst, P. M. Pardalos, and N. V. Thoai, "Introduction to global optimization," in *Nonconvex Optimization and Its Applications*. Norwell, MA: Kluwer, 1995, vol. 3.
- [13] S. S. Rao, *Engineering Optimization: Theory and Practice*, 3rd ed. New York: Wiley, 1996.
- [14] P. Y. Papalambros and D. J. Wilde, *Principles of Optimal Design: Modeling and Computation*, 2nd ed. Cambridge, U.K.: Cambridge Univ. Press, 2000.
- [15] R. L. Haupt, "Introduction to genetic algorithms for electromagnetics," *IEEE Antennas Propagat. Mag.*, vol. 37, pp. 7–15, Apr. 1995.
- [16] J. M. Johnson and Y. Rahmat-Samii, "Genetic algorithms in engineering electromagnetics," *IEEE Antennas Propagat. Mag.*, vol. 39, pp. 7–25, Aug. 1997.
- [17] D. E. Goldberg, *Genetic Algorithms in Search, Optimization, and Machine Learning*. Reading, MA: Addison-Wesley, 1989.
- [18] E. Aarts and J. Korst, *Simulated Annealing and Boltzmann Machines: A Stochastic Approach to Combinatorial Optimization and Neural Computing*. New York: Wiley, 1989.

- [19] L. Davis, Ed., *Genetic Algorithms and Simulated Annealing*. New York: Pitman, 1987.
- [20] S. Kirkpatrick, C. D. Gelatt, Jr., and M. P. Vecchi, "Optimization by simulated annealing," *Science*, vol. 220, no. 4598, pp. 671–680, 1983.
- [21] N. Metropolis, A. Rosenbluth, M. Rosenbluth, A. Teller, and E. Teller, "Equation of state calculations by fast computing machines," *J. Chem. Phys.*, vol. 21, no. 6, pp. 1087–1092, 1953.
- [22] A. E. W. Jones and G. W. Forbes, "An adaptive simulated annealing algorithm for global optimization over continuous variables," *J. Global Optimiz.*, vol. 6, no. 1, pp. 1–37, Jan. 1995.
- [23] H. S. Tsai, M. J. W. Rodwell, and R. A. York, "Planar amplifier array with improved bandwidth using folded-slots," *IEEE Microwave Guided Wave Lett.*, vol. 4, pp. 112–114, Apr. 1994.
- [24] H. S. Tsai and R. A. York, "Applications of planar multiple-slot antennas for impedance control, and analysis using FDTD with Berenger's PML method," in *Proc. IEEE Antennas Propagat. Soc. Int. Symp.*, vol. 1, 1995, pp. 370–373.
- [25] R. Coccioli, W. R. Deal, and T. Itoh, "Radiation characteristics of a patch antenna on a thin PBG substrate," in *Proc. IEEE Antennas Propagat. Soc. Int. Symp.*, Atlanta, GA, 1998, pp. 656–659.
- [26] J. S. Colburn and Y. Rahmat-Samii, "Patch antennas on externally perforated high dielectric constant substrates," *IEEE Trans. Antennas Propagat.*, vol. 47, pp. 1785–1794, Dec. 1999.
- [27] H. Contopanagos, L. Zhang, and N. G. Alexopoulos, "Thin frequency-selective lattices integrated in novel compact MIC, MMIC, and PCA architectures," *IEEE Trans. Microwave Theory Tech.*, vol. 46, pp. 1936–1948, Nov. 1998.



Zhifang Li (S'96–M'02) was born in China, in 1972. She received the B.S. degree in mathematics from Peking University, Beijing, China, in 1995. She received the dual M.S. degrees in electrical engineering and computer engineering and the Ph.D. degree in electrical engineering from the University of Michigan, Ann Arbor, in 1996, 1999, and 2001, respectively.

From 1995 to 2001, she was a Graduate Research Assistant with the Radiation Laboratory and the Optimal Design Laboratory at the University of

Michigan. She is currently a Senior Electrical Engineer with e Guidant Corporation in St. Paul, MN. Her research interests include numerical techniques in electromagnetics and use of optimization methods in the design of patch antennas and periodic structures.



Yunus E. Erdemli (S'96–M'02) was born in Tatvan, Turkey, in 1970. He received the B.S. degree in electrical engineering from Middle East Technical University, Ankara, Turkey, and the M.S. and Ph.D. degrees from the University of Michigan, Ann Arbor, both in electrical engineering, in 1992, 1996, and 2002, respectively.

In 1992, he joined Turkish Military Electronics, Inc., Ankara, Turkey, as an RF Design Engineer. From 1994 to 2002, he was a Graduate Research Assistant at the University of Michigan Radiation

Laboratory, Ann Arbor, where he is currently a Postdoctoral Research Fellow. His research interests include numerical-analysis and design of conformal/reconfigurable arrays and frequency-selective surfaces/volumes for broad-band applications, model order reduction algorithms for electromagnetics, and electromagnetic coupling studies in automobile vehicles.

In 1994, Dr. Erdemli was awarded the Abroad Ph.D. Fellowship by The Higher Educational Council of Turkey and was sponsored by Kocaeli University, Izmit, Turkey, until 2000.



John L. Volakis (S'77–M'82–SM'89–F'96) was born in Chios, Greece, in 1956. He received the B.E. degree, *summa cum laude*, from Youngstown State University, Youngstown, OH, and the M.Sc. and Ph.D. degrees, both from The Ohio State University, Columbus, OH, in 1978, 1979, and 1982, respectively.

From 1978 to 1982, he was a Graduate Research Associate at The Ohio State University Electro-Science Laboratory. From 1982 to 1984, he was with Rockwell International, Aircraft Division.

Since 1984, he has been with the University of Michigan, Ann Arbor, where he is currently a Professor in the Department of Electrical Engineering and Computer Science (EECS). From 1998 to 2000, he served as the Director of the Radiation Laboratory, also at the University of Michigan. His primary research interests include the development and application of computational and design techniques to scattering, antennas, and bioelectromagnetics. He has published over 180 articles in major refereed journal articles (9 of these have appeared in reprint volumes), more than 220 conference papers, and nine book chapters. In addition, he coauthored two books: *Approximate Boundary Conditions in Electromagnetics* (Piscataway, NJ: IEEE Press, 1995) and *finite-element method for Electromagnetics* (Piscataway, NJ: IEEE Press, 1998).

Dr. Volakis received the University of Michigan College of Engineering Research Excellence Award in 1998 and the Department of Electrical Engineering and Computer Science Service Excellence Award in 2001. He served as an Associate Editor of the IEEE TRANSACTIONS ON ANTENNAS AND PROPAGATION from 1988 to 1992; as an Associate Editor of *Radio Science* from 1994 to 1997; chaired the 1993 IEEE Antennas and Propagation Society Symposium and Radio Science Meeting, and was a member of the AdCom for the IEEE Antennas and Propagation Society from 1995 to 1998. He now serves as associate editor for the *Journal of Electromagnetic Waves and Applications*, the IEEE ANTENNAS AND PROPAGATION SOCIETY MAGAZINE, and the *URSI Bulletin*. He is a member of Sigma Xi, Tau Beta Pi, Phi Kappa Phi, and Commission B of URSI. He is also listed in several Who is Who directories, including *Who is Who in America*.



Panos Y. Papalambros received the diploma in mechanical and electrical engineering degree from the National Technical University of Athens, Greece, and the M.S. and Ph.D. degrees from Stanford University, Palo Alto, CA, in 1974, 1976, and 1979, respectively.

He is currently the Donald C. Graham Professor of Engineering and a Professor of Mechanical Engineering and the Executive Director of the Automotive Research Center at the University of Michigan, Ann Arbor. Since 1979, he has been at the University of Michigan, where he served as Department Chair

from 1992 to 1998 and as founding director of several laboratories and centers. His research interests include design methods and optimization, with applications to automotive systems, and product development. With D. J. Wilde, he coauthored the textbook *Principles of Optimal Design: Modeling and Computation* (Cambridge: U.K.: Cambridge Univ. Press, 1988, 2000).

Dr. Papalambros is a Fellow of ASME. In 1998, he received the ASME Design Automation Award, and in 1999, he received the ASME Machine Design Award.